Published online 6 September 2021

Nucleic Acids Research, 2021, Vol. 49, No. 17 ***9809–9820***
https://doi.org/10.1093/nar/gkab758

Reciprocal stabilization of transcription factor binding integrates two signaling pathways to regulate fission yeast *fbp1* transcription

Wakana Koda[1,†], Satoshi Senmatsu[1,†], Takuya Abe[1], Charles S. Hoffman[2] and Kouji Hirota[1,*]

[1]Department of Chemistry, Graduate School of Science, Tokyo Metropolitan University, Minamiosawa 1-1, Hachioji-shi, Tokyo 192-0397, Japan and [2]Biology Department, Boston College, Chestnut Hill, MA 02467, USA

Received April 15, 2021; Revised July 27, 2021; Editorial Decision August 16, 2021; Accepted August 29, 2021

ABSTRACT

Transcriptional regulation, a pivotal biological process by which cells adapt to environmental fluctuations, is achieved by the binding of transcription factors to target sequences in a sequence-specific manner. However, how transcription factors recognize the correct target from amongst the numerous candidates in a genome has not been fully elucidated. We here show that, in the fission-yeast *fbp1* gene, when transcription factors bind to target sequences in close proximity, their binding is reciprocally stabilized, thereby integrating distinct signal transduction pathways. The *fbp1* gene is massively induced upon glucose starvation by the activation of two transcription factors, Atf1 and Rst2, mediated via distinct signal transduction pathways. Atf1 and Rst2 bind to the upstream-activating sequence 1 region, carrying two binding sites located 45 bp apart. Their binding is reciprocally stabilized due to the close proximity of the two target sites, which destabilizes the independent binding of Atf1 or Rst2. Tup11/12 (Tup-family co-repressors) suppress independent binding. These data demonstrate a previously unappreciated mechanism by which two transcription-factor binding sites, in close proximity, integrate two independent-signal pathways, thereby behaving as a hub for signal integration.

INTRODUCTION

Transcriptional control is essential to all organisms to adapt to environmental change. Transcriptional aberrations are related to serious diseases, including cancer (1). Investigating transcriptional regulatory mechanisms is therefore an important area of research. The transcriptional response of the proper gene at the proper time is accomplished by the regulation of transcription-factor (TF) binding. TF binding status determines which genes are activated or repressed and when (2,3). However, how TFs search for and recognize their target sequences from among the numerous candidate sites in a huge genome has not been fully elucidated.

Chromatin structure, including the position of nucleosomes, is important to the control of transcription. TF-binding status is linked to open-chromatin regions where positioned nucleosomes are not formed, since positioned nucleosomes interfere with TF access to DNA (4,5). Dissociation and/or sliding of nucleosomes mediates open chromatin and thus leads to TF-binding and transcriptional activation. Conversely, some TFs (referred to as pioneer TFs) initially bind to target sites in nucleosome-formed heterochromatin, thereby inducing open-chromatin configurations around their binding motifs and allowing access to newly arrived TFs (6–8). Thus, the local chromatin structure is closely linked to TF binding and plays a pivotal role in transcriptional regulation.

In the fission yeast *Schizosaccharomyces pombe*, transcription of the *fbp1* gene, which encodes fructose-1,6-bisphosphatase, an essential enzyme for gluconeogenesis, is massively activated in response to glucose starvation (9,10). Transcription of *fbp1* is activated by two TFs: the CREB/ATF type TF Atf1 and the C_2H_2 zinc-finger type TF Rst2 (11,12). Atf1 and Rst2 bind to *fbp1* upstream cis-acting elements called upstream activating sequences 1 and 2 (UAS1 and UAS2), respectively (12). UAS1 includes a cAMP response element, while UAS2 includes a stress response element (12). These sites are located 627 bp apart in the *fbp1* upstream region.

The two TFs, Atf1 and Rst2, are regulated through distinct-signaling pathways. Under glucose starvation stress, Atf1 is phosphorylated and activated by the Spc1/Sty1 mitogen-activated protein kinase (MAPK) pathway (13–15). Rst2 is activated under glucose starvation by the inactivation of protein-kinase A (PKA) via the

*To whom correspondence should be addressed. Tel: +81 42 677 2542; Fax: +81 42 677 2542; Email: khirota@tmu.ac.jp
†The authors wish it to be known that, in their opinion, the first two authors should be regarded as Joint First Authors.

repression by the PKA-regulatory subunit, Cgs1, following depletion of cellular cAMP (11,16–18). In addition to these regulatory mechanisms, Tup-family co-repressors Tup11 and Tup12 play critical roles in *fbp1* regulation (19–23). However, the relationship between the TFs and the Tup11/12 co-repressors remains uncertain. We previously demonstrated that Rst2 is initially recruited to a CT-rich binding motif located 45 bp upstream from the Atf1-binding site (UAS1) and subsequently delivered to UAS2 through a local-loop structure during the early stages of *fbp1* transcription (20). Thus, Rst2 and Atf1 initially bind to a region where the two binding sites are in close proximity. We herein define this region as the 'UAS1 region,' which carries two binding motifs located 45 bp apart (Figure 1A).

In this study, we demonstrate that Atf1 and Rst2 interdependently bind to the UAS1 region in close proximity. The Tup11/12 co-repressors suppress the independent binding of Atf1 or Rst2, but this interdependent binding of the two TFs counteracts this suppression. This study demonstrates how two TF-binding motifs in close proximity can facilitate the integration of distinct signaling pathways and thereby serve as a hub for signal integration.

MATERIALS AND METHODS

Fission yeast strains, genetic methods and cell culture

The fission yeast strains used in this study are listed in Supplementary Table S1. Yeast-extract-repression (YER) medium (yeast extract containing 6% glucose) and yeast-extract-derepression (YED) medium (yeast extract containing 0.1% glucose and 3% glycerol) supplemented with adenine (50 μg/ml) were used for cell culture under glucose-rich and starvation conditions, respectively. Transformation was carried out using the lithium-acetate method, as described previously (24). Standard genetic procedures were carried out as described previously (25). To select kanamycin-resistant and uracil-auxotrophic colonies, culture suspensions were inoculated onto plates containing yeast extract (YE) and 2% glucose, incubated for 16 h, then replica-plated onto YE plates containing 100 μg/ml G-418 sulfate (Wako) and SD plates containing 100 μg/ml uracil and 1 mg/ml of 5-FOA (Wako), respectively.

Primers

Primer sequences are shown in Supplementary Table S2.

Construction of *Insertion-100 bp* and *Insertion-300 bp* strains

To insert a 100 or 300 bp *act1* sequence between the two TF-binding sites in the *fbp1* UAS1 region, we amplified three fragments, act1-core, fbp1-left and fbp1-right, using primers P1 and P2 or P3, P4 and P5, and P6 or P7 and P8, respectively (Supplementary Table S2.). The resultant fragments, fbp1-left and fbp1-right, carry sequences flanked by 20 bp *act1* sequences. The fragments were purified using a QIAquick gel extraction kit (Qiagen). The three DNA fragments were jointed and amplified using primers P4 and P8 and cloned using a Zero Blunt™TOPO™PCR Cloning kit (Thermo Fisher Scientific). Introduction of insertions was confirmed by sequencing using primer P31. PCR amplification using these plasmids together with primers P4 and P8 produced products used to target changes to the *fbp1* chromosomal locus. A strain carrying a *ura4* selection-marker gene at the *fbp1* upstream region *Hpa*I site was transformed to 5FOA-resistance due to the loss of *ura4* with the PCR products. Insertion of the *act1* sequence was confirmed by PCR using primers P9 and P10. We confirmed the insertion of these sequences by the direct sequence analysis of amplified fragments using primer P31.

Construction of *Insertion-5, 10, 15 and 20 bp* strains

To insert a 5, 10, 15 or 20 bp *act1* sequence between the two TF-binding sites in the *fbp1* UAS1 region, we amplified two fragments, fbp1-left and fbp1-right carrying short *act1* sequences (5, 10, 15 or 20 bp) at their flanking sequence, using primers P4/P32 and P8/P33 (for 5 bp), P4/P34 and P8/P35 (for 10 bp), P4/P36 and P8/P37 (for 15 bp), or P4/P38 and P8/P39 (for 20 bp), respectively (Supplementary Table S2). The fragments were purified using a QIAquick gel extraction kit (Qiagen). The two DNA fragments were joined and amplified using primers P4 and P8 phosphorylated by T4 Polynucleotide Kinase (Takara) and cloned into the *EcoRV* site in pBlueScript II SK (–). Introduction of insertions was confirmed by sequencing using primer P31. PCR amplification using these plasmids together with primers P4 and P8 produced products used to target changes to the *fbp1* chromosomal locus. A strain carrying a *ura4* selection-marker gene at the *fbp1* upstream region HpaI site was transformed to 5-FOA-resistance due to the loss of *ura4* with the PCR products. Insertion of the *act1* sequence was confirmed by PCR using primers P9 and P10. We confirmed the insertion of these sequences by the direct sequence analysis of amplified fragment.

Construction of *tupΔΔ* strains

To construct the *tup11*Δ/*tup12*Δ/*Insertion-100 bp* and *tup11*Δ/*tup12*Δ/*Insertion-300 bp* strains, the *tup11::ura4* locus was amplified using primers P11 and P12, after which the *Insertion-100 bp* and *Insertion-300 bp* strains were transformed with the resultant PCR product and selected for uracil prototrophy using SD plates lacking uracil. To further disrupt the *tup12* gene, the genome sequence containing *tup12* was amplified using primers P13 and P14 and cloned into pBlueScript II SK (+). The resulting plasmid was digested at the HindIII site within *tup12* and a *LEU2* cassette was introduced to generate the Tup12::LEU2 plasmid. The *tup12*::*LEU2* sequence was amplified from this plasmid using primers P15 and 16 and used to disrupt *tup12*. The *tup11*Δ strains, derived from either *Insertion-100 bp* or *Insertion-300 bp*, were transformed with the PCR product and selected for leucine prototrophy. To confirm *tup*ΔΔ, *tup11* and *tup12* loci were amplified using primers P17 to 18 and P19 to 20, respectively.

Construction of *rst2-3flag* strains

All *rst2-3flag* strains were constructed as described previously (26).

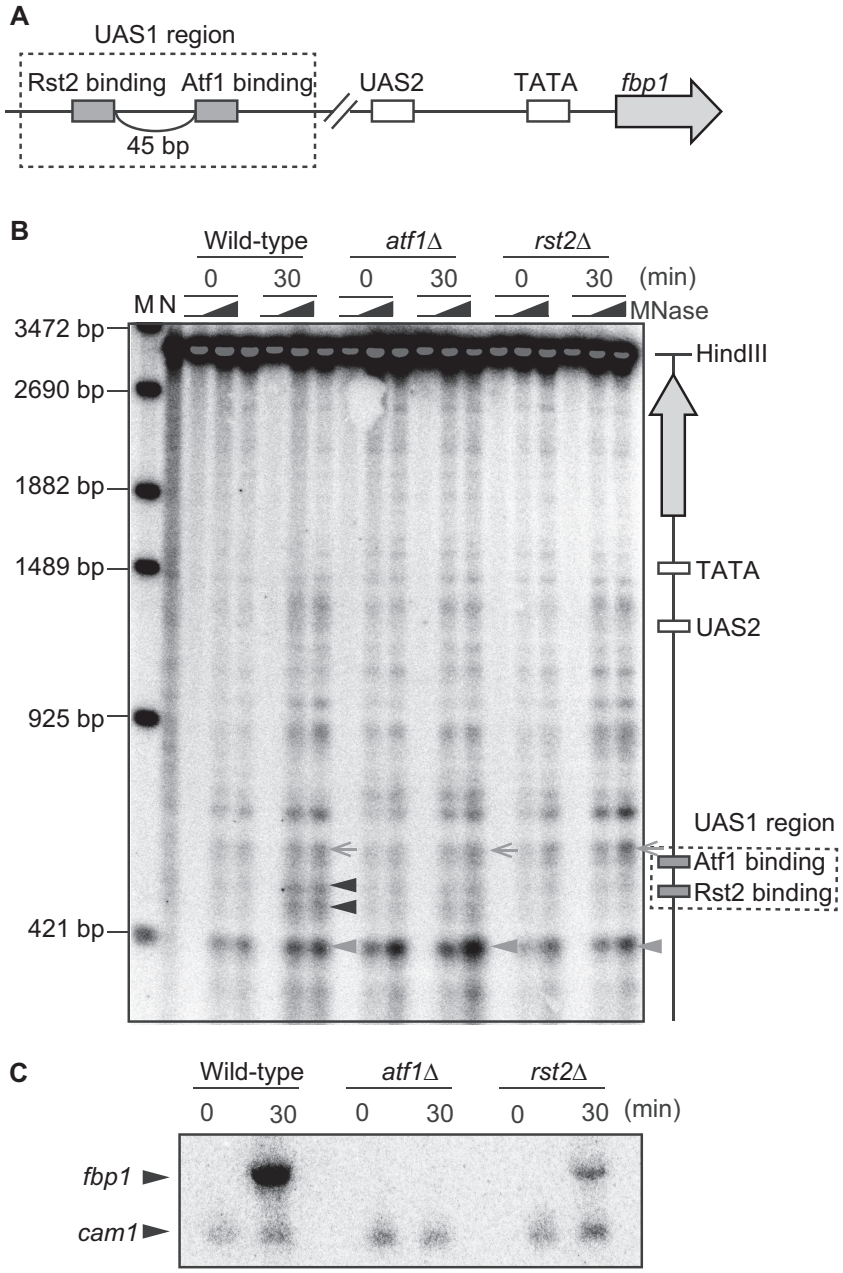

Figure 1. Both Atf1 and Rst2 are required for chromatin opening around the UAS1 region. (**A**) Schematic representation of TF-binding sites in the *fbp1* promoter. The Atf1- and Rst2-binding sites are located 45 bp apart in the UAS1 region. (**B**) The chromatin structure upstream from the *fbp1* gene was analyzed by an MNase-digestion assay in wild-type, *atf1*Δ and *rst2*Δ cells. Lane N represents the partial digestion of naked DNA with MNase. Lane M represents the size marker (λEcoT14I, Takara Bio). The indicated cells were cultured in YER medium (+glucose; 0 min), then transferred to YED medium (–glucose) and cultured for 30 min. The extracted chromatin DNA was partially digested by MNase 0, 20 and 50 U/ml at 37°C (from left lane). The purified DNA was digested by HindIII, followed by Southern blot analysis to detect the MNase-sensitive sites. Black arrowheads represent MNase sensitive sites induced by glucose starvation, while the gray arrow and arrowhead represent constitutive MNase sensitive sites around the UAS1 region. Quantitative data for the intensity of MNase sensitive bands is shown in Supplementary Figure S1. (**C**) *fbp1* transcription was examined by northern blot analysis in wild-type, *atf1*Δ, and *rst2*Δ cells. Cells were cultured as in (B). The *cam1* transcript was used as an internal control (45).

Northern blot and indirect end-labeling analysis using MNase-digested chromatin DNA

Northern blot and MNase digestion assays were performed as described previously (27). For the MNase digestion assay, a DNA probe for the HindIII-end was prepared using the Megaprime™ DNA Labeling System (GE Health Care) and a PCR fragment as a template. PCR was performed using primers P21 and P22.

Chromatin immunoprecipitation (ChIP) and qPCR

Chromatin immunoprecipitation coupled with quantitative PCR (ChIP-qPCR) was performed as previously described using anti-Atf1 (abcam ab18123) and Anti-DYKDDDDK (Wako 018-22383) antibody (20,28). For the detection of the UAS1 region, Atf1-binding site, Rst2-binding site, and Prp3-ORF, primers P23 and P24, P25 and P26, P27 and P28, P29 and P30 were used, respectively.

Sequential ChIP analysis

Fifty milliliters of culture was incubated with 37% formaldehyde (1.4 ml) solution for 20 min at room temperature, after which 2.5 M glycine (2.5 ml) was added and incubated for 5 min. After centrifugation, collected cells were washed twice with ice-cold TBS buffer (150 mM NaCl, 20mM Tris–HCl [pH 7.5]). The cells were mixed with lysis 140 buffer (400 μl) (0.1% Na-deoxycholate, 1 mM EDTA, 50 mM HEPES–KOH [pH 7.5], 140 mM NaCl and 1% Triton X100) and zirconia beads (0.6 ml) were added. After disruption of cells using a multi-beads shocker (Yasuikikai, Osaka, Japan), the suspension was sonicated 6 times for 30 s each to shear chromosomal DNA into fragments (about 500 bp) and centrifuged at 4°C, after which the supernatant was collected as a whole-cell extract. The recommended amount of antibodies (anti-Atf1 [abcam ab18123] and Anti-DYKDDDDK [Wako 018-22383]) according to the specifications provided by the manufacturer, and DYNA-protein A beads (20 μl) (DYNAL, Oslo, Norway) were mixed at 4°C overnight to conjugate antibodies and beads. Whole-cell extract (300 μl) was mixed with pretreated Anti-DYKDDDDK-beads complex and allowed to immunoprecipitate overnight at 4°C. The precipitates were washed twice with lysis 140 buffer and once with lysis 500 (0.1% Na-deoxycholate, 1 mM EDTA, 50 mM HEPES–KOH [pH 7.5], 500 mM NaCl and 1% Triton X100), then washed a further two times with wash buffer (0.5% Na-deoxycholate, 1 mM EDTA, 250 mM LiCl, 0.5% NP-40, and 10 mM Tris–HCl [pH 8.0]), then washed a final time with TE (10 mM Tris–HCl [pH 8.0] and 1 mM EDTA). The well-washed precipitates were mixed with TBS buffer (100 μl) containing 5 mg/ml of 3-FLAG peptide (Sigma) and held at room temperature for 30 min to allow for the elution of co-precipitant. Eluted materials were diluted by lysis 140 buffer (300 μl) and mixed with pretreated Anti-Atf1-beads complex and allowed to immunoprecipitate overnight at 4°C. The precipitates were washed as described above and allowed to elute the immunoprecipitated protein-DNA complexes in elution buffer (40 μl) (10 mM EDTA 1% SDS and 50 mM Tris–HCl [pH 8.0]) at 65°C for 10 min. The samples were then mixed with TE buffer (250 μl) containing 1% SDS and 63 μg of proteinase K (Merck, Darmstadt, Germany) and incubated at 37°C for 16 h. After incubation, the temperature was shifted to 65°C and the samples were incubated for a further 6 h. After incubation, DNA was phenol/chloroform extracted from each of the samples.

Next-generation sequence analysis of sequential ChIP samples

The above-described sequential-ChIP samples, including input DNA, ChIP control samples (ChIP without antibodies), and sequential-ChIP samples (pulled down with α-Atf1 and α-Flag antibodies), were used for next-generation sequence analysis. We prepared a library from the eluted DNA samples using the NEBNext Ultra II FS DNA Library Prep Kit for Illumina (NEB, MA) with the END repair/dA-tailing module and Index primers (NEB, MA). Sequencing was conducted by Eurofins Genomics (Eurofins Scientific, Luxembourg). Read-mapping was carried out as previously described (29). The sequential-ChIP seq data are available at DDBJ Sequence Read Archive (DRA) (https://www.ddbj.nig.ac.jp/dra/index.html, accession number: DRA011814).

RESULTS

Atf1 and Rst2 are required for chromatin opening in the UAS1 region

The UAS1 region carries binding sites for Atf1 and Rst2, which are located 45 bp apart from each other (Figure 1A). To examine the involvement of these TFs in the regulation of local chromatin configuration in the UAS1 region during *fbp1* transcriptional activation, we employed indirect end-labeling analysis using micrococcal-nuclease (MNase)-digested chromatin to reveal nuclease-hypersensitive sites, which reflect an open chromatin configuration. To investigate the position of MNase-sensitive sites in the UAS1 region, we set the probe near a HindIII site that is located 241 bp from the Atf1-binding site in the UAS1 region. In wild-type cells, two prominent MNase-sensitive sites appeared around the UAS1 region under glucose starvation (i.e. at 30 min) (Figure 1B, black arrowheads) between two constitutive MNase sensitive sites (Figure 1B, gray arrow and arrowhead). In marked contrast, *atf1*Δ and *rst2*Δ cells exhibited less-prominent, MNase-sensitive bands around the UAS1 region upon glucose starvation (Figure 1B). The distribution of the band intensity is shown in Supplementary Figure S1. Moreover, loss of Atf1 completely eliminated *fbp1* expression, while loss of Rst2 reduced, but did not completely eliminate, *fbp1* expression (Figure 1C). Such reduced *fbp1* expression in *rst2*Δ cells has been detected at later time-points after glucose starvation (11,22), thus the reduction in *fbp1* expression in *rst2*Δ cells seen here is not simply a reflection of delayed kinetics. These data indicate that both Atf1 and Rst2 are required for chromatin opening around UAS1 region and activation of *fbp1* mRNA transcription.

Activation of both Atf1 and Rst2 is required for chromatin opening in the UAS1 region

We next sought to examine the activation requirements of both TFs: Atf1 and Rst2. Atf1 and Rst2 are regulated by distinct-signal pathways, the MAPK and PKA pathways, respectively. Atf1 is phosphorylated and activated by a MAPK, Spc1 (13–15), while Rst2 is activated by the suppression of PKA via the PKA-regulatory subunit Cgs1 (11,16,18). To determine if activation of both TFs is required for chromatin opening in the UAS1 region, we examined chromatin opening in *spc1*Δ and *cgs1*Δ cells. As with the *atf1*Δ and *rst2*Δ cells, both *spc1*Δ and *cgs1*Δ cells exhibited a less-prominent MNase-sensitive site under glucose starvation (Figure 2A, black arrowheads) between two constitutive MNase sensitive sites (Figure 2A, gray arrow and arrowhead), compared to wild-type cells. The distribution of the band intensity is shown in Supplementary Figure S2. Moreover, both *spc1*Δ and *cgs1*Δ cells exhibited defects in *fbp1* mRNA induction (Figure 2B). These data suggest that activation of both TFs via distinct-signaling pathways is essential for chromatin opening in the UAS1 region and activation of *fbp1* mRNA transcription.

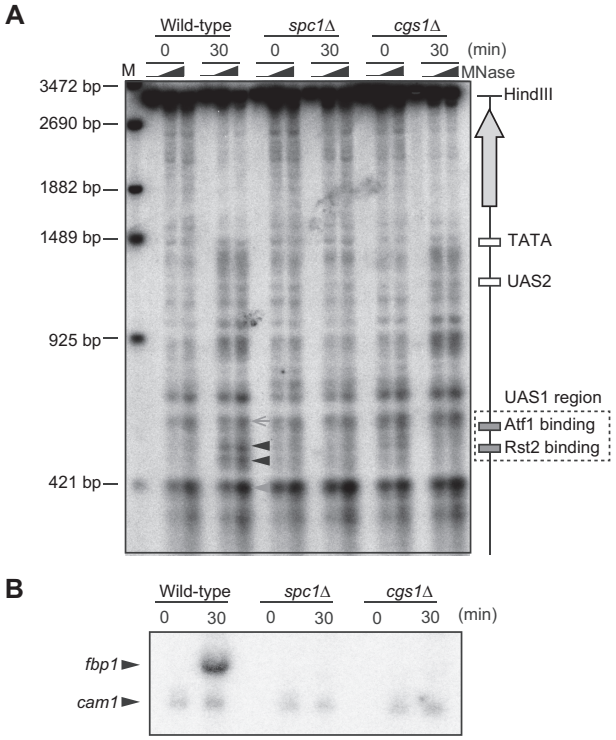

Figure 2. Activation of both Atf1 and Rst2 is pivotal for chromatin opening around the UAS1 region. (**A**) The chromatin structure was assessed as in Figure 1B in wild-type, *spc1*Δ and *cgs1*Δ cells. Lane M represents the size marker (λEcoT14I, Takara Bio). Black arrowheads represent MNase sensitive sites induced by glucose starvation, while the gray arrow and arrowhead represent constitutive MNase sensitive sites around the UAS1 region. Quantitative data for the intensity of MNase sensitive bands is shown in Supplementary Figure S2. (**B**) *fbp1* transcription was examined as in Figure 1C in wild-type, *spc1*Δ and *cgs1*Δ cells.

Atf1 and Rst2 interdependently bind to the UAS1 region

Having established that activation of both Atf1 and Rst2 is required for chromatin opening in the UAS1 region, we posited a possible collaboration between Atf1 and Rst2 binding to the UAS1 region. To test this assumption, we examined both Atf1 and Rst2 binding to the UAS1 region via chromatin-immunoprecipitation (ChIP) analysis. In wild-type cells, the binding of Atf1 and Rst2 to the UAS1 region was increased under glucose starvation (Figure 3A), while binding of Atf1 and Rst2 to the UAS1 region was significantly reduced in *rst2Δ* and *atf1Δ* cells, respectively (Figure 3A). Thus, Atf1 is indispensable for the stable binding of Rst2 to the UAS1 region, while Rst2 enhances binding of Atf1 to this region. We next examined the binding of Atf1 and Rst2 to the UAS1 region in cells carrying a mutation in either the Rst2 binding CT-rich sequence (Rst2 binding-mut) cells (20) or the Atf1 binding CRE sequence (Atf1 binding-mut) cells (12), respectively. As with the *rst2*Δ and *atf1*Δ cells, binding of Atf1 and Rst2 to the UAS1 region was significantly reduced in Rst2 binding-mut and Atf1 binding-mut cells (Figure 3B). These data indicate that Atf1 and Rst2 bind to the UAS1 region in an interdependent manner and further suggest that they reciprocally stabilize binding.

Close proximity of the two binding motifs is required for the interdependent binding of Atf1 and Rst2 to the UAS1 region

To test whether or not the close proximity of Atf1 and Rst2 in the UAS1 region is required for the reciprocal stabilization of their binding, we examined the effect of increasing the distance between the two TF binding sites. To this end, we inserted 100 bp or 300 bp of *act1* sequence between the Rst2 and Atf1-binding sites and generated *Insertion-100 bp* or *Insertion-300 bp* strains, respectively (Figure 4A). An *act1* ORF sequence was used as a neutral sequence carrying no TF-binding activity (30,31). We examined the effect of these changes on chromatin remodeling in the UAS1 region. As we previously showed, wild-type cells displayed two prominent MNase-sensitive sites in the UAS1 region upon glucose starvation (Figure 4B, black arrowheads) between the constitutive MNase sensitive sites (Figure 4B, gray arrow and arrowheads). The distribution of the band intensity is shown in Supplementary Figure S3. Note that in this experiment, we observed that the Rst2-binding site corresponds to the two prominent MNase-sensitive sites that appear in the wild-type cells (Figure 4B, black arrowheads), while the Atf1-binding site showed a constitutive open-chromatin configuration (Figure 4B, gray arrow). In the *Insertion-100bp* and *Insertion-300 bp* strains, the intensity of the two MNase-sensitive sites around the Rst2-binding site was markedly reduced (Figure 4B and C). The distributions of the band intensity are shown in Supplementary Figure S3. These results indicate that close proximity of the two binding motifs is required for efficient chromatin opening at the Rst2-binding site in the UAS1 region. Moreover, induction of *fbp1*-mRNA was reduced as the distance between the two TF-binding sites increased, indicating that close proximity is pivotal for efficient *fbp1* induction. (Figure 4D, Supplementary Figure S4).

The significance of close proximity between the two TF-binding sites in the UAS1 region led us to hypothesize that Atf1 and Rst2 bind to adjacent sites and stabilize each other's binding. To test this hypothesis, we examined the binding status of Atf1 and Rst2 in the insertion mutants. Efficiency of Atf1 binding to the UAS1 region was gradually reduced as the distance between the two TF-binding sites increased (Figure 4E). Strikingly, efficiency of Rst2 binding to the UAS1 region was critically impaired by the 100 bp-insertion (Figure 4E). In sum, these data indicate that stable binding of both Atf1 and Rst2 depends upon the two binding sites being in close proximity, and further suggests that independent binding of these TFs is destabilized by some mechanism(s).

Loss of Tup11/12 bypasses the close-proximity requirement of the two TF-binding sites for stable TF-binding to the UAS1 region

We hypothesized that the transcriptional co-repressors Tup11 and Tup12 (Tup11/12) might be involved in the destabilization of independent TF-binding to the UAS1 region, since these co-repressors play a role in the destabilization of the independent binding of Rst2 to UAS2, and the delivery of Rst2 from the UAS1 region via local genome-loop structure counteracts this destabilization (20). To test this assumption, we examined the role of Tup11/12

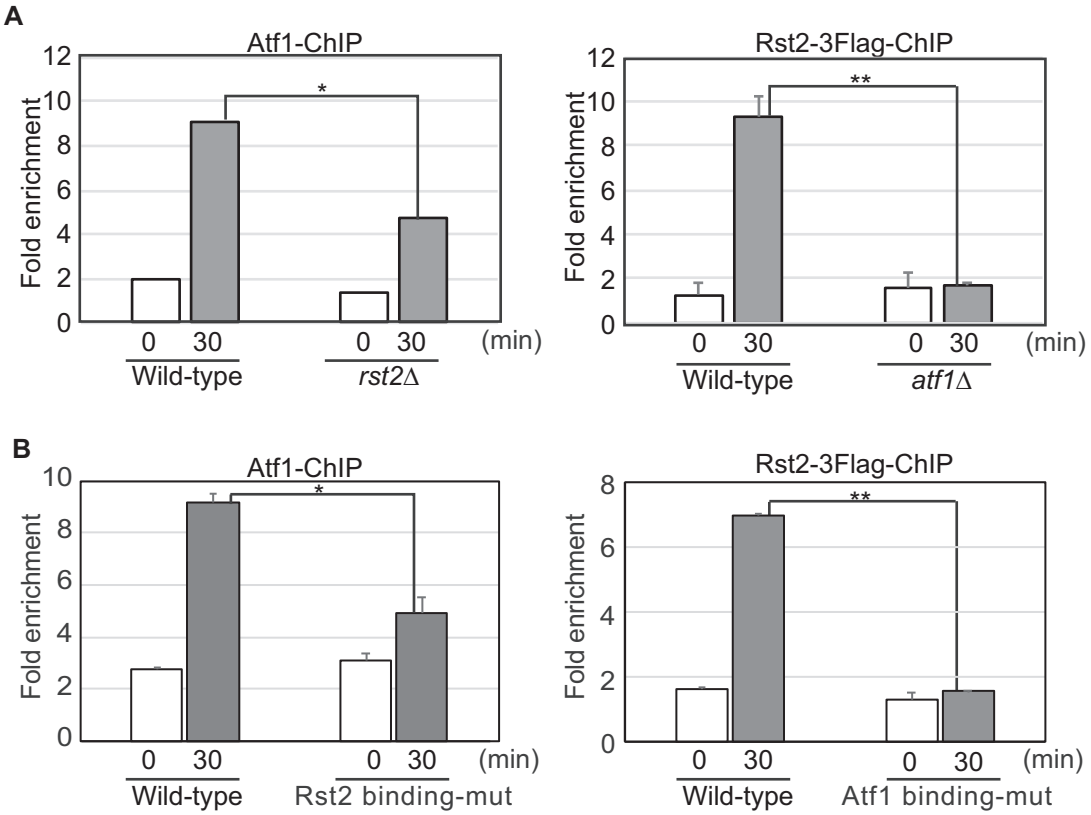

Figure 3. Atf1 and Rst2 interdependently bind to the UAS1 region. (A, B) Binding of Atf1 and Rst2-3flag to the UAS1 region in wild-type, *rst2*Δ, and *atf1*Δ cells (**A**) and wild-type, Atf1 binding-mut, and Rst2 binding-mut cells (**B**) was examined by ChIP analysis. Cells were cultured as in Figure 1B. ChIP signals were quantified by qPCR as described in Materials and Methods. ChIP signals for the *prp3* open-reading frame (ORF) were used for normalization. Error bars represent standard deviation from two independent experiments. Statistical significance (Student's *t*-test) was as follows: $^{*}P < 0.05$, $^{**}P < 0.01$.

in TF-binding destabilization by generating *tup11*Δ *tup12*Δ (*tup*ΔΔ) strains from the insertion-mutant strains (Figure 4A), and measuring TF binding to the UAS1 region, as was done in Figure 4E. As expected, loss of Tup11/12 (*tup11*/*tup12*–/–) augmented binding of Atf1 and Rst2 in wild-type cells (Figure 5A, insertion 0 bp), which is consistent with the role played by the Tup superfamily co-repressors in the repression of TF recruitment (20,32,33). More importantly, loss of Tup11/12 significantly restored binding of Atf1 and Rst2 to their target sites in *Insertion-100 bp* and *Insertion-300 bp* strains (Figure 5A, insertion 100 and 300 bp). Likewise, loss of Tup11/12 significantly rescued transcriptional defects of *fbp1* mRNA in *Insertion-100 bp* and *Insertion-300 bp* strains (Figure 5B). These results suggest that Tup11/12 destabilizes binding of Atf1 and Rst2 to the UAS1 region and that concurrent binding of these TFs in close proximity counteracts this destabilization. Should this be the case, the loss of Tup11/12 might also suppress the defects of TF-binding in *atf1*Δ and *rst2*Δ cells. To test this possibility, we measured TF binding to the UAS1 region in *atf1*Δ, *atf1*Δ/*tup11*/*tup12*Δ, *rst2*Δ and *rst2*Δ/*tup11*/*tup12*Δ cells. Similar to the data shown in Figure 3, loss of Rst2 significantly reduced the binding of Atf1 to the UAS1 region (Figure 6A). Concurrent loss of Tup11/12 in *rst2*Δ cells significantly augmented Atf1 binding to near the level observed in wild-type cells (Figure 6A, $P < 0.05$). Similarly, in the absence of Tup11/12, the Atf1 requirement for Rst2 binding to the UAS1 region was significantly bypassed (Figure 6A, $P < 0.05$). Defects in *fbp1* mRNA activation in *atf1*Δ and *rst2*Δ cells were also consistently rescued by the loss of Tup11/12 (Figure 6B, C). These data indicate that Tup11/12 destabilizes and represses individual binding of these TFs, whereas reciprocal stabilization of these TFs in close proximity counteracts this repression.

Importance of relative helical positions of the two TF-binding sites in the reciprocal stabilization of TFs

If two TFs binding within proximity stabilize each other, the relative helical position of these binding sites may also affect binding stabilization. To test this hypothesis, we inserted 5, 10, 15, or 20 bp *act1* sequences between the Atf1 and Rst2 binding sites in UAS1 region and generated *Inserion-5 bp*, *Inserion-10 bp*, *Inserion-15 bp*, or *Inserion-20 bp* cells, respectively. As a right-handed double helix in B-DNA contains ∼10 bp per turn (34), the 5 and 15 bp insertions, but not 10 and 20 bp insertions, might affect the relative helical position of two TF binding sites (Supplementary Figure S5A). The expression of *fbp1* was significantly reduced in *Inserion-5 bp* and *Inserion-15 bp* cells but not in *Inserion-10bp* or *Inserion-20 bp* cells (Supplementary Figure S5B, C). Consistently, *Inserion-5 bp* and *Inserion-15 bp* cells, but not *Inserion-10 bp* or *Inserion-20 bp* cells, exhibited reduced binding of Rst2 in UAS1 region

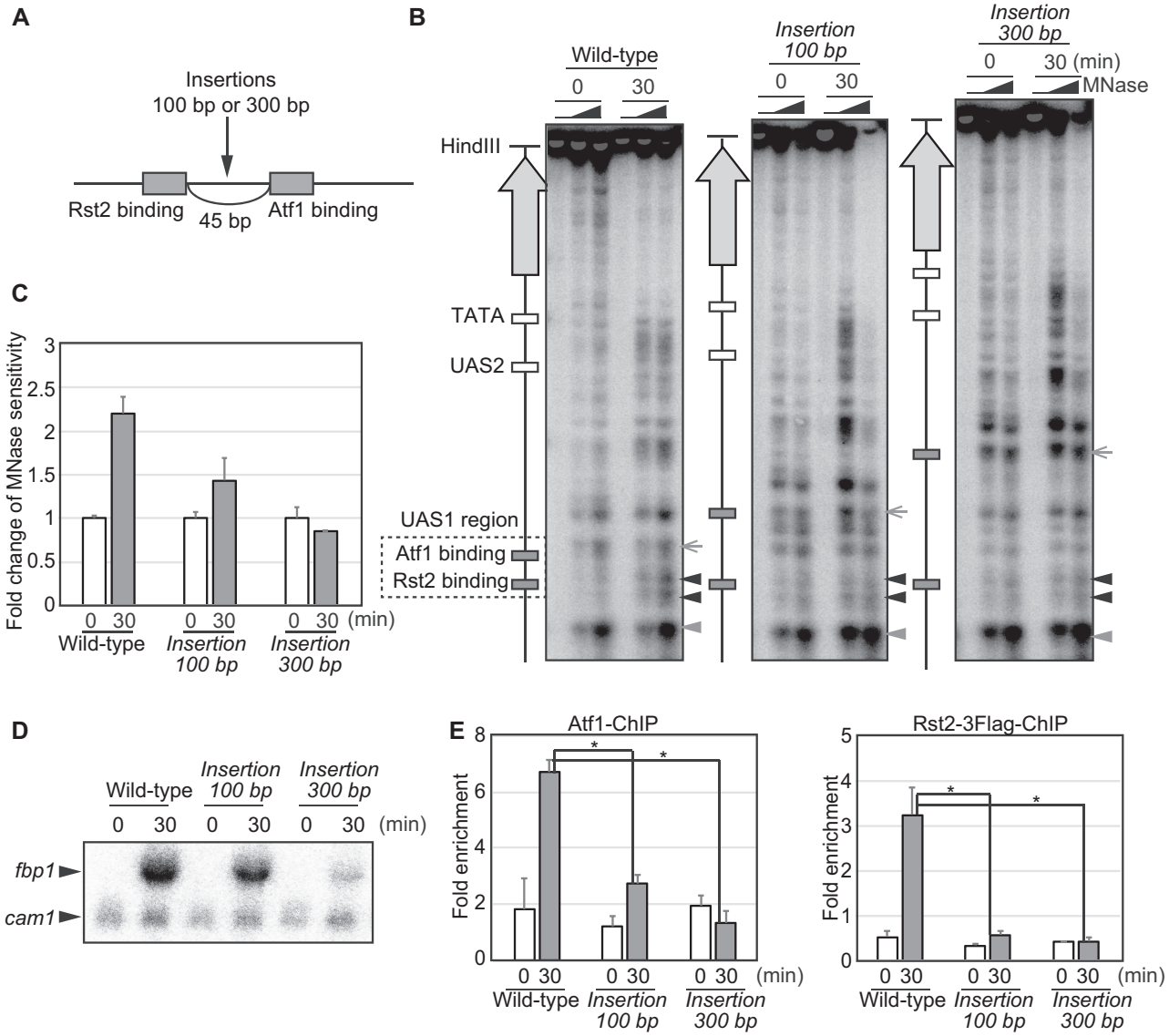

Figure 4. Close proximity of two binding motifs is required for the stable binding of Atf1 and Rst2 to the UAS1 region. (**A**) Schematic representation of the UAS1 region in *Insertion-100 bp* and *Insertion-300 bp* strains. 100 or 300 bp of the *act1* ORF fragment was inserted between the Atf1 and Rst2-binding sites. (**B**) Chromatin structure was analyzed by MNase-digestion assay as in Figure 1B in wild-type, *Insertion-100bp*, and *Insertion-300 bp* cells. Black arrowheads represent MNase sensitive sites induced by glucose starvation, while the gray arrow and arrowhead represent constitutive MNase sensitive sites around the UAS1 region. Quantitative data for the distributions of the band intensity of MNase sensitive sites are shown in Supplementary Figure S3. (**C**) Bar charts represent quantification of the MNase-sensitive bands shown in B. Band intensity was quantified using Image J (https://imagej.nih.gov/ij/). Error bars represent standard deviation from two independent experiments. (**D**) *fbp1* transcription was examined in the indicated cells as in Figure 1C. Quantitative data for *fbp1* transcription level are shown in Supplementary Figure S4. (**E**) Separation of the TF-binding sites impairs TF-binding to the UAS1 region. Binding of Atf1 and Rst2-3flag to the Atf1 or Rst2-binding sites in the UAS1 region was examined in the indicated cells using specific primers. Error bars represent standard deviation from two independent experiments. Statistical significance (Student's *t*-test) was as follows: $^{*}P < 0.05$.

(Supplementary Figure S5D). The binding of Atf1 was maintained in *Inserion-5 bp* cells, but reduced in *Inserion-15 bp* cells (Supplementary Figure S5D). These modest effects on the Atf1 binding might be due to the fact that Rst2 is not essential for the binding of Atf1 (Figure 3). These results suggest that relative helical position of two TF-binding sites is also important for their reciprocal stabilization. In sum, the UAS1 region might serve as a hub for signal integration through strict binding suppression and interdependent binding of TFs.

Genome-wide analysis of sequences to which Atf1 and Rst2 concurrently bind

Having established that the UAS1 region in *fbp1* plays a role as a hub for signal integration via strict binding suppression and interdependent TF-binding, we wished to identify other genomic regions to which Atf1 and Rst2 interdependently bind under glucose starvation. To this end, we co-precipitated genomic DNA to which Atf1 and Rst2 concurrently bind with sequential-ChIP analysis using anti-Flag and anti-Atf1 antibodies in *rst2-3flag* cells,

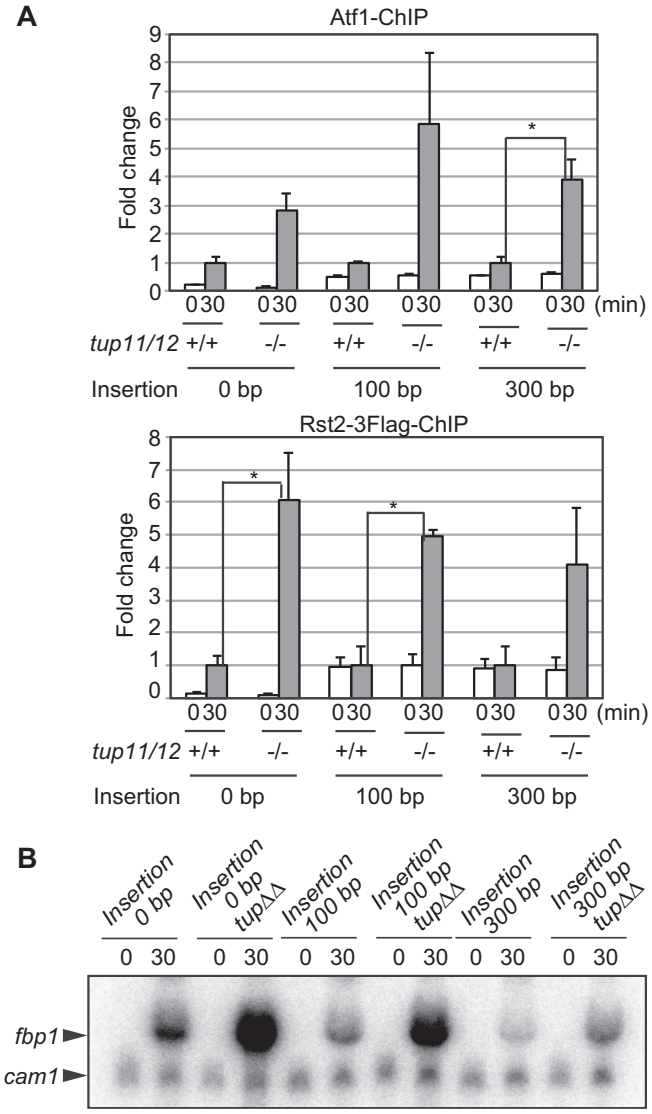

Figure 5. Loss of Tup11/12 bypasses the close-proximity requirement for stable TF-binding to the UAS1 region. (**A**) Binding of Atf1 and Rst2-3flag to the Atf1 and Rst2-binding sites in the UAS1 region was examined in the indicated cells as in Figure 4E. Error bars represent standard deviations. The experiment was performed twice and the mean and standard deviation were calculated. The mean value of the induced state of *Tup11/12*+/+ cells was then set to 1 to present relative changes in the ratio to induced condition in the *tup11/12*+/+ cells. Statistical significance (Student's *t*-test) was as follows: $^{*}P < 0.05$. (**B**) *fbp1* transcription was examined in the indicated cells as in Figure 1C.

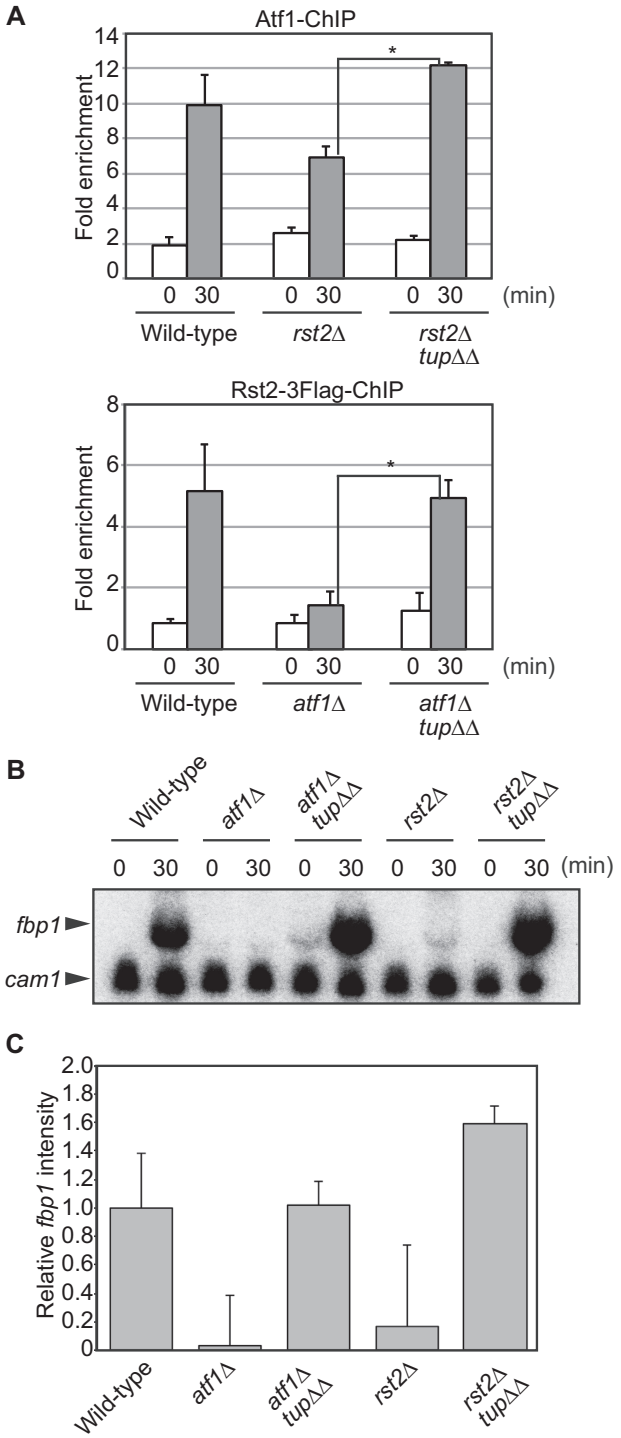

Figure 6. Loss of Tup11/12 bypasses the requirement of concurrent binding of Atf1 and Rst2 to UAS1 region. (**A**) Binding of Atf1 and Rst2-3flag to the UAS1 region was examined in the indicated cells as in Figure 3. Error bars represent standard deviation from two independent experiments. Statistical significance (Student's *t*-test) was as follows: $^{*}P < 0.05$. (**B**) *fbp1* transcription was examined in the indicated cells as in Figure 1C. (**C**) *fbp1* mRNA transcripts were quantified using ImageJ (https://imagej.nih.gov/ij/) and intensities at 30 min after glucose starvation relative to those of *tup11/12*+/+ cells are presented. Error bars represent standard deviation from two independent experiments.

and analyzed the resultant ChIP DNA samples via next-generation sequencing. The sequence-reads mapped in the whole-fission genome are presented in Supplementary Figure S6. We used MACS2 2.1.2 (https://github.com/macs3-project/MACS) to identify peaks from the mapped-read data. There were 536 and 837 peaks in the glucose-rich and glucose-starved ChIP samples, respectively, while only 27 and 26 peaks in the glucose-rich and glucose-starved ChIP control samples (IP without antibodies), respectively. We detected the *fbp1* UAS1 region by this analysis

(Figure 7A, arrow). We explored the highly-enriched (in comparison to input) and highly-augmented (glucose starved) regions and found the *ght4* hexose transporter gene upstream region using these criteria (Figure 7B, arrow). The *ght4* upstream region has been previously identified as one of the Tup11/12 binding regions (35). Moreover, Atf1 binding to this region is affected by Tup11/12 (35). In the *ght4* upstream region, we found two sequences arranged in tandem containing both putative CRE (Atf1-binding site) and CT-rich sequences (Rst2 binding sequence) that are located 33 and 42 bp apart, respectively (Figure 7C, shaded). We next addressed a possible collaboration between Atf1 and Rst2 in binding to this region. In wild-type cells, binding of Atf1 and Rst2 to the *ght4* upstream region was increased under glucose starvation (Figure 7D). Binding of Atf1 and Rst2 to this region was significantly reduced in the *rst2Δ* and *atf1Δ* cells, respectively, indicating that Atf1 and Rst2 bind to the *ght4* upstream region in an interdependent manner (Figure 7D). Consistently, *ght4* was massively induced under glucose starvation, but such induction was weaker in the *rst2Δ* and *atf1Δ* cells (Figure 7E). These results again demonstrate that genomic regions containing adjacent CRE (Atf1-binding site) and CT-rich (Rst2 binding sequence) sequences can act as hubs for signal integration in *S. pombe*.

DISCUSSION

In this study, we investigated the mechanisms that integrate the activity of TFs regulated by distinct-signaling pathways onto their target genomic sequences in the fission yeast *fbp1* gene. Our study demonstrates that two TFs, Atf1 and Rst2, both pivotal factors for *fbp1* transcription regulated through distinct signaling pathways, interdependently bind to the UAS1 region in the *fbp1* promoter and induce chromatin opening in this region. This interdependent TF binding is facilitated by the proximity of the two TF-binding motifs, which are located 45 bp apart from each other. The Tup-family co-repressors Tup11 and Tup12 play a role in the repression of the independent binding of Atf1 and Rst2, while the concurrent binding of Atf1 and Rst2 in close proximity counteracts this repression. The present data suggest that concurrent activation of Atf1 and Rst2 through distinct-signaling pathways permits their stable binding to the UAS1 region; thus this region acts as a hub for signal integration (Supplementary Figure S7).

The essential binding sites for Atf1 and Rst2 in the *fbp1* promoter are UAS1 and UAS2, respectively (12). We previously demonstrated that Rst2 binds to the UAS1 region in the initial stage of transcriptional activation and is subsequently delivered to UAS2 (20). We posit that *fbp1* transcription is tightly controlled through rigorous TF regulation in terms of specificity and timing via a two-step mechanism: signal integration in the UAS1 region during the initial stage, and recruitment and delivery of Rst2 to the UAS2 region after chromatin opening. In this study, we demonstrate that the mechanism that integrates the signaling pathways on the genomic sequence, is dependent upon the close proximity of the two TF-binding motifs, with the recruited TFs stabilizing each other, in fission yeast.

In the UAS1 region, the binding sites for Atf1 and Rst2 are located 45 bp apart from each other. We conjecture the following mechanism for reciprocal-binding stabilization: First, activated Atf1 starts to bind to the target site in the UAS1 region, since this site has a constitutively open chromatin configuration (Figure 4). Second, Rst2 access may be enhanced by the local influence of the chromatin configuration at the Rst2-binding site in the UAS1 region via the adjacent Atf1 binding. Third, Rst2 binding might further open the surrounding chromatin, thereby enhancing the binding stability of both TFs. Should this be the case, activation of both Atf1 and Rst2 would be a prerequisite for the stable binding of both, as well as chromatin remodeling. This is indeed the case, as the loss of the upstream essential factors required for the activation of Atf1 or Rst2 critically impaired chromatin opening in the UAS1 region in *fbp1* transcriptional activation (Figures 1 and 2). In addition to this mechanism, TF binding might be further stabilized by the following mechanism: two TFs might directly interact and stabilize each other. This possibility is supported by the fact that the distance between the two TF binding sites (45 bp) equals ∼15 nm, which is approximately the predicted total size of Atf1 (60 kDa, 6 nm in a diameter) and Rst2 (62 kDa, 6 nm in a diameter) based on their molecular weights. Thus, it is possible that the two TFs in close proximity directly stabilize each other's binding. Conservation of such reciprocal TF-binding stabilization in the other eukaryotic cells is supported by the observation that significant cooperativity among 113 TFs has been identified in budding yeast cells (36). Moreover, a recent report shows that most human TFs bind to sequences that are bound by more than one type of TF, suggesting significant TF-TF cooperation (37). Our current study may add mechanistic insight into such TF–TF cooperation: (i) reciprocal stabilization of TFs in close proximity and (ii) destabilization of independent binding of TFs by Tup-family co-repressors, Tup11 and Tup12.

The Tup-family global co-repressor is conserved in flies, worms, and mammals. Budding yeast Tup1 represses a wide range of stress-responsive genes by establishing silent chromatin via recruitment of histone deacetylase and/or by directly repressing the general transcriptional machinery (38–42). Budding yeast Tup1 can also directly regulate transcription by masking and inhibiting the transcriptional activation domain of the recruited proteins (43). Moreover, *S. cerevisiae* Tup1, *S. pombe* Tup11/12, and mouse ortholog Grg3 also repress the binding of TFs to their target sites (20,32,33). In fission-yeast cells, Tup11/12 co-repressors distribute throughout the *fbp1* upstream regulatory region, with peaks at UAS1 and UAS2, and such binding is enhanced during *fbp1* activation (19,26). In this study, we revealed the previously unappreciated repression mechanism by which independent binding of Atf1 or Rst2 to the UAS1 region is destabilized, with activation and binding of both TFs in close proximity counteracting this repression. Tup11/12 is thus pivotal for the function of the UAS1 region as a hub for signal integration. Tup11/12 is known to play a pivotal role in the stress-specific transcriptional response of stress-responsive genes, including *fbp1*, by repressing the non-specific alteration of chromatin (21,44). We propose that Tup11/12 is not a simple repressor and has broader functions, as demonstrated in this study. One

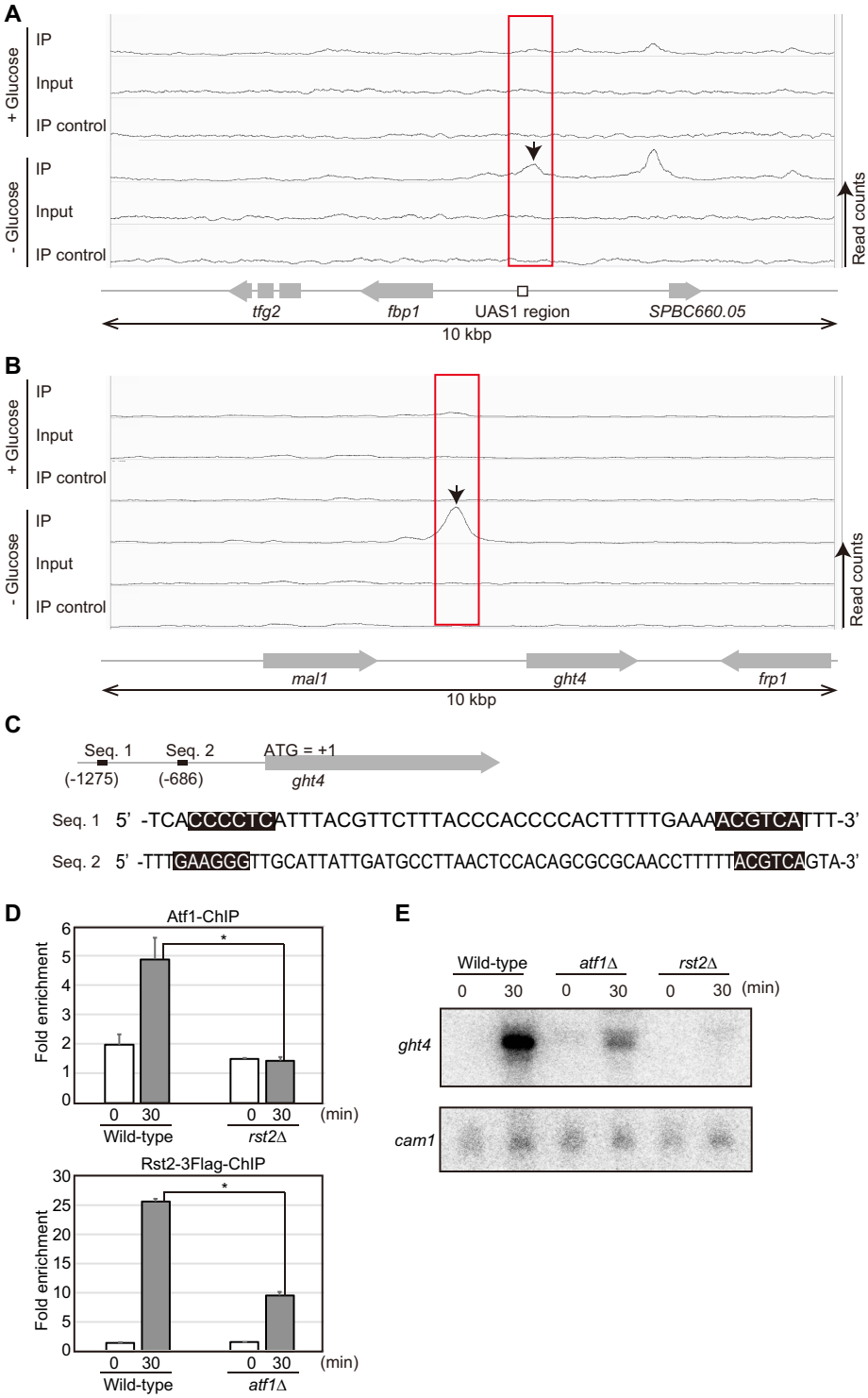

Figure 7. Genome-wide analysis of sequences where Atf1 and Rst2 concurrently bind. (**A**) Sequential-ChIP seq profile for Atf1 and Rst2 in the UAS1 region of *fbp1*. Data were visualized using the integrative genome viewer IGV, version 2.5.1 (https://software.broadinstitute.org/software/igv/). The Atf1-Rst2 peak with increased occupancy under glucose starvation is indicated by the arrow in the rectangle. IP (sequential-ChIP samples pulled down with α-Atf1 and α-Flag antibodies), Input (whole cell extract), and IP control (sequential-ChIP samples pulled down without antibody) were analyzed. (**B**) Sequential-ChIP seq profile for Atf1 and Rst2 in the *ght4* upstream region. Data were visualized as in (A). The Atf1-Rst2 peak, with increased occupancy under glucose starvation, is indicated by the arrow in the rectangle. (**C**) Two sequences (seq. 1 and seq. 2) in tandem containing putative CRE sequence (shaded) and CT-rich sequence (shaded) in the *ght4* upstream region. The numbers indicate the position of these sequences from the first ATG of the *ght4* open reading frame. (**D**) Binding of Atf1 and Rst2-3flag to the *ght4* upstream region in wild-type, *rst2*Δ, and *atf1*Δ cells was examined by ChIP analysis. Cells were cultured as in Figure 1B. ChIP signals were quantified by qPCR. ChIP signals for the *prp3* open-reading frame (ORF) were used for normalization. Error bars represent standard deviation from two independent experiments. Statistical significance (Student's *t*-test) was as follows: $^{*}P < 0.05$. (**E**) *ght4* transcription was examined in the indicated cells as in Figure 1C.

possible mechanism for this Tup11/12-mediated, stress-specific response in *fbp1* is as follows: Tup11/12 represses the binding of TFs to both the UAS1 region and to UAS2, and both TF-binding sites are placed in close proximity via the formation of the local loop structure (20), resulting in highly specific and ordered TF-binding. Identifying how Tup11/12 governs this stress-specific response would further assist us to understand this important transcriptional-response mechanism.

DATA AVAILABILITY

The sequential-ChIP seq data are available at DDBJ Sequence Read Archive (DRA) (https://www.ddbj.nig.ac.jp/dra/index.html, accession number: DRA011814).

SUPPLEMENTARY DATA

Supplementary Data are available at NAR Online.

ACKNOWLEDGEMENTS

We thank all members of our laboratory for their help. We also thank the staff at the Radioisotope Research Center, Tokyo Metropolitan University, for their support in the use of isotopes.

FUNDING

JSPS KAKENHI [JP21K19235, JP20H04337, JP19KK0210, JP16H01314 to K.H., JP19J20773 to S.S.]; Yamada Science Foundation; Takeda Science Foundation (to K.H.). Funding for open access charge: Takeda Science Foundation.
Conflict of interest statement. None declared.

REFERENCES

1. Wouters,J., Kalender Atak,Z. and Aerts,S. (2017) Decoding transcriptional states in cancer. *Curr. Opin. Genet. Dev.*, **43**, 82–92.
2. Deplancke,B., Alpern,D. and Gardeux,V. (2016) The genetics of transcription factor DNA binding variation. *Cell*, **166**, 538–554.
3. MacQuarrie,K.L., Fong,A.P., Morse,R.H. and Tapscott,S.J. (2011) Genome-wide transcription factor binding: beyond direct target regulation. *Trends Genet.*, **27**, 141–148.
4. Wolffe,A.P. (1994) Nucleosome positioning and modification: chromatin structures that potentiate transcription. *Trends Biochem. Sci.*, **19**, 240–244.
5. Wolffe,A.P. (1997) Histones, nucleosomes and the roles of chromatin structure in transcriptional control. *Biochem. Soc. Trans.*, **25**, 354–358.
6. Mayran,A. and Drouin,J. (2018) Pioneer transcription factors shape the epigenetic landscape. *J. Biol. Chem.*, **293**, 13795–13804.
7. Mayran,A., Sochodolsky,K., Khetchoumian,K., Harris,J., Gauthier,Y., Bemmo,A., Balsalobre,A. and Drouin,J. (2019) Pioneer and nonpioneer factor cooperation drives lineage specific chromatin opening. *Nat. Commun.*, **10**, 3807.
8. Zaret,K.S. and Carroll,J.S. (2011) Pioneer transcription factors: establishing competence for gene expression. *Genes Dev.*, **25**, 2227–2241.
9. Hoffman,C.S. and Winston,F. (1990) Isolation and characterization of mutants constitutive for expression of the fbp1 gene of Schizosaccharomyces pombe. *Genetics*, **124**, 807–816.
10. Hoffman,C.S. and Winston,F. (1991) Glucose repression of transcription of the *Schizosaccharomyces pombe* fbp1 gene occurs by a cAMP signaling pathway. *Genes Dev.*, **5**, 561–571.
11. Higuchi,T., Watanabe,Y. and Yamamoto,M. (2002) Protein kinase A regulates sexual development and gluconeogenesis through phosphorylation of the Zn finger transcriptional activator Rst2p in fission yeast. *Mol. Cell. Biol.*, **22**, 1–11.
12. Neely,L.A. and Hoffman,C.S. (2000) Protein kinase A and mitogen-activated protein kinase pathways antagonistically regulate fission yeast fbp1 transcription by employing different modes of action at two upstream activation sites. *Mol. Cell. Biol.*, **20**, 6426–6434.
13. Kanoh,J., Watanabe,Y., Ohsugi,M., Iino,Y. and Yamamoto,M. (1996) Schizosaccharomyces pombe gad7+ encodes a phosphoprotein with a bZIP domain, which is required for proper G1 arrest and gene expression under nitrogen starvation. *Genes Cells*, **1**, 391–408.
14. Shiozaki,K. and Russell,P. (1996) Conjugation, meiosis, and the osmotic stress response are regulated by Spc1 kinase through Atf1 transcription factor in fission yeast. *Genes Dev.*, **10**, 2276–2288.
15. Wilkinson,M.G., Samuels,M., Takeda,T., Toone,W.M., Shieh,J.C., Toda,T., Millar,J.B. and Jones,N. (1996) The Atf1 transcription factor is a target for the Sty1 stress-activated MAP kinase pathway in fission yeast. *Genes Dev.*, **10**, 2289–2301.
16. Yamamoto,M., Imai,Y. and Watanabe,Y. (1997) In: Prigle,J.R., Broach,J.R. and Jones,E.W. (eds). *Mating and Sporulation in Schizosaccharomyces Pombe. The Molecular and Cellular Biology of the yeast Saccharomyces*. Cold Spring Habor Laboratory Press, NY, pp. 1037–1196.
17. Gupta,D.R., Paul,S.K., Oowatari,Y., Matsuo,Y. and Kawamukai,M. (2011) Multistep regulation of protein kinase A in its localization, phosphorylation and binding with a regulatory subunit in fission yeast. *Curr. Genet.*, **57**, 353–365.
18. Kunitomo,H., Higuchi,T., Iino,Y. and Yamamoto,M. (2000) A zinc-finger protein, Rst2p, regulates transcription of the fission yeast ste11(+) gene, which encodes a pivotal transcription factor for sexual development. *Mol. Biol. Cell*, **11**, 3205–3217.
19. Asada,R., Takemata,N., Hoffman,C.S., Ohta,K. and Hirota,K. (2015) Antagonistic controls of chromatin and mRNA start site selection by Tup family corepressors and the CCAAT-binding factor. *Mol. Cell. Biol.*, **35**, 847–855.
20. Asada,R., Umeda,M., Adachi,A., Senmatsu,S., Abe,T., Iwasaki,H., Ohta,K., Hoffman,C.S. and Hirota,K. (2017) Recruitment and delivery of the fission yeast Rst2 transcription factor via a local genome structure counteracts repression by Tup1-family corepressors. *Nucleic. Acids. Res.*, **45**, 9361–9371.
21. Hirota,K., Hasemi,T., Yamada,T., Mizuno,K.I., Hoffman,C.S., Shibata,T. and Ohta,K. (2004) Fission yeast global repressors regulate the specificity of chromatin alteration in response to distinct environmental stresses. *Nucleic. Acids. Res.*, **32**, 855–862.
22. Hirota,K., Hoffman,C.S., Shibata,T. and Ohta,K. (2003) Fission yeast Tup1-like repressors repress chromatin remodeling at the fbp1+ promoter and the ade6-M26 recombination hotspot. *Genetics*, **165**, 505–515.
23. Janoo,R.T., Neely,L.A., Braun,B.R., Whitehall,S.K. and Hoffman,C.S. (2001) Transcriptional regulators of the Schizosaccharomyces pombe fbp1 gene include two redundant Tup1p-like corepressors and the CCAAT binding factor activation complex. *Genetics*, **157**, 1205–1215.
24. Hirota,K., Tanaka,K., Watanabe,Y. and Yamamoto,M. (2001) Functional analysis of the C-terminal cytoplasmic region of the M-factor receptor in fission yeast. *Genes Cells*, **6**, 201–214.
25. Gutz,H., Heslot,H., Leupold,U. and Loprieno,N. (1974) In: *Handbook of genetics*. Plenum Press, NY, Vol. **1**, pp. 395–446.
26. Hirota,K., Hoffman,C.S. and Ohta,K. (2006) Reciprocal nuclear shuttling of two antagonizing Zn finger proteins modulates Tup family corepressor function to repress chromatin remodeling. *Eukaryot Cell*, **5**, 1980–1989.
27. Hirota,K., Fukuda,T., Yamada,T. and Ohta,K. (2009) Analysis of chromatin structure at meiotic DSB sites in yeasts. *Methods Mol. Biol.*, **557**, 253–266.
28. Umeda,M., Tsunekawa,C., Senmatsu,S., Asada,R., Abe,T., Ohta,K., Hoffman,C.S. and Hirota,K. (2018) Histone Chaperone Asf1 Is Required for the Establishment of Repressive Chromatin in Schizosaccharomyces pombe fbp1 Gene Repression. *Mol. Cell. Biol.*, **38**, e00194-18.
29. Oda,A., Takemata,N., Hirata,Y., Miyoshi,T., Suzuki,Y., Sugano,S. and Ohta,K. (2015) Dynamic transition of transcription and

chromatin landscape during fission yeast adaptation to glucose starvation. *Genes Cells*, **20**, 392–407.
30. Senmatsu,S., Asada,R., Abe,T., Hoffman,C.S., Ohta,K. and Hirota,K. (2019) lncRNA transcriptional initiation induces chromatin remodeling within a limited range in the fission yeast fbp1 promoter. *Sci. Rep.*, **9**, 299.
31. Senmatsu,S., Asada,R., Oda,A., Hoffman,C.S., Ohta,K. and Hirota,K. (2021) lncRNA transcription induces meiotic recombination through chromatin remodelling in fission yeast. *Commun Biol*, **4**, 295.
32. Buck,M.J. and Lieb,J.D. (2006) A chromatin-mediated mechanism for specification of conditional transcription factor targets. *Nat. Genet.*, **38**, 1446–1451.
33. Sekiya,T. and Zaret,K.S. (2007) Repression by Groucho/TLE/Grg proteins: genomic site recruitment generates compacted chromatin in vitro and impairs activator binding in vivo. *Mol. Cell*, **28**, 291–303.
34. Wang,J.C. (1979) Helical repeat of DNA in solution. *Proc. Natl. Acad. Sci. U.S.A.*, **76**, 200–203.
35. Takemata,N., Oda,A., Yamada,T., Galipon,J., Miyoshi,T., Suzuki,Y., Sugano,S., Hoffman,C.S., Hirota,K. and Ohta,K. (2016) Local potentiation of stress-responsive genes by upstream noncoding transcription. *Nucleic Acids Res.*, **44**, 5174–5189.
36. Banerjee,N. and Zhang,M.Q. (2003) Identifying cooperativity among transcription factors controlling the cell cycle in yeast. *Nucleic Acids Res.*, **31**, 7024–7031.
37. Nie,Y., Shu,C. and Sun,X. (2020) Cooperative binding of transcription factors in the human genome. *Genomics*, **112**, 3427–3434.
38. Courey,A.J. and Jia,S. (2001) Transcriptional repression: the long and the short of it. *Genes Dev.*, **15**, 2786–2796.
39. Davie,J.K., Edmondson,D.G., Coco,C.B. and Dent,S.Y. (2003) Tup1-Ssn6 interacts with multiple class I histone deacetylases in vivo. *J. Biol. Chem.*, **278**, 50158–50162.
40. Malavé,T.M. and Dent,S.Y. (2006) Transcriptional repression by Tup1-Ssn6. *Biochem. Cell. Biol.*, **84**, 437–443.
41. Smith,R.L. and Johnson,A.D. (2000) Turning genes off by Ssn6-Tup1: a conserved system of transcriptional repression in eukaryotes. *Trends Biochem. Sci.*, **25**, 325–330.
42. Zhang,Z. and Reese,J.C. (2004) Ssn6-Tup1 requires the ISW2 complex to position nucleosomes in *Saccharomyces cerevisiae*. *EMBO J.*, **23**, 2246–2257.
43. Wong,K.H. and Struhl,K. (2011) The Cyc8-Tup1 complex inhibits transcription primarily by masking the activation domain of the recruiting protein. *Genes Dev.*, **25**, 2525–2539.
44. Greenall,A., Hadcroft,A.P., Malakasi,P., Jones,N., Morgan,B.A., Hoffman,C.S. and Whitehall,S.K. (2002) Role of fission yeast Tup1-like repressors and Prr1 transcription factor in response to salt stress. *Mol. Biol. Cell*, **13**, 2977–2989.
45. Takeda,T. and Yamamoto,M. (1987) Analysis and in vivo disruption of the gene coding for calmodulin in Schizosaccharomyces pombe. *Proc. Natl. Acad. Sci. U.S.A.*, **84**, 3580–3584.